Unified approach for nucleon knock-out and coherent and incoherent pion production in neutrino interactions with nuclei

M. Martini,[1,2,3] M. Ericson,[1,3] G. Chanfray,[1] and J. Marteau[1]
[1]*Université de Lyon, Univ. Lyon 1, CNRS/IN2P3, IPN Lyon, F-69622 Villeurbanne Cedex, France*
[2]*Università di Bari, I-70126 Bari, Italy*
[3]*Theory Group, Physics Department, CERN, CH-1211 Geneva, Switzerland*
(Received 17 October 2009; published 23 December 2009)

We present a theory of neutrino interactions with nuclei aimed at the description of the partial cross sections, namely quasielastic and multinucleon emission, coherent and incoherent single-pion production. For this purpose, we use the theory of nuclear responses treated in the random-phase approximation, which allows a unified description of these channels. It is particularly suited for the coherent pion production where collective effects are important, whereas they are moderate in the other channels. We also study the evolution of the neutrino cross sections with the mass number from carbon to calcium. We compare our approach to the available neutrino experimental data on carbon. We put a particular emphasis on the multinucleon channel, which at present is not easily distinguishable from the quasielastic events. This component turns out to be quite relevant for the interpretation of experiments (K2K, MiniBooNE, SciBooNE). It can account in particular for the unexpected behavior of the quasielastic cross section.

DOI: 10.1103/PhysRevC.80.065501 PACS number(s): 25.30.Pt, 13.15.+g, 24.10.Cn, 25.40.−h

I. INTRODUCTION

Neutrino physics has undergone a spectacular development in the past decade, following the discovery of neutrino oscillations first revealed by the anomaly of atmospheric neutrinos [1]. A number of results on the interaction of neutrinos with matter are now available. Neutrino detectors do not usually consist of pure hydrogen but they involve complex nuclei, for instance, ^{12}C, as in SciBar [2], where the molecule C_8H_8 is involved, or in MiniBooNE [3], which uses the mineral oil CH_2. Heavier nuclei are also under consideration, for instance, in the liquid argon chamber planned for T2K [4,5]. A number of results have been obtained for neutral or charged current (K2K, MiniBooNE, SciBooNE) on quasielastic processes or coherent and incoherent single-pion production [6–17]. The first question is then if our present understanding of neutrino interactions with matter can reproduce the available data. Many works [18–36] have been devoted to this problem, using various theoretical approaches [37–64]. In this article we will explore such interactions using the theory of the nuclear response treated in the random-phase approximation (RPA) in the quasielastic and Δ resonance region including also two and three nucleon knock-out. The formalism is the same as the one used by Marteau [38] in his work on the ν-^{16}O interaction. The merit of this approach is that, although perfectible in several ways, it describes in a unique frame several final-state channels. This technique has been successful in a number of problems involving either weakly interacting probes such as (e, e') scattering or strongly interacting ones such as pion scattering or (^{3}He,T) charge exchange reaction [65]. We give the cross sections for pion production, coherent or incoherent, and nucleon knock-out, for neutral or charged currents. We restrict to single-pion production ignoring two-pion production processes that, for real photons, lead to a sizable part of the photoabsorption cross section at energies larger than the Δ resonance, above $\simeq$500 MeV. Our treatment should thus underestimate the cross section when multipion production starts to show up. Our work ignores as well the meson exchange effects that play a non-negligible role [66,67]. We take into account only the exchange effect in the time component of the axial current, which is known to be important [68]. For single-pion production we assume that the dominant production mechanism is via the Δ resonance, ignoring the other resonance excitations, which also limits the energy for the validity of our approach. Beyond quasielastic processes and single-pion production via Δ excitation we also incorporate several nucleon knock-out through two-particle-two-hole (2p-2h) and 3p-3h excitations. These will play a crucial role in the comparison with data involving quasielastic events.

Among the aims of this work there is the exploration of the evolution of the neutrino-nucleus interaction as the mass number of the nucleus goes from the carbon region to the region of ^{40}Ca. This investigation is motivated by the project of a liquid argon chamber in the T2K experiment that raises the question if one keeps control of the understanding of the interaction of neutrinos with matter by going to a medium-weight nucleus such as ^{40}Ar. In order to single out the evolutions linked to the nuclear size we have chosen as element of comparison an isoscalar nucleus in the ^{40}Ar region, namely ^{40}Ca. For the coherent process that per nucleon fades away in heavy nuclei, the evolution is relatively rapid but should remain under control as our theory is particularly well adapted to this channel. The other exclusive channels, in particular the incoherent pion production, are sensitive to final-state interaction not automatically included in our approach. This leaves some uncertainty in the evolution between the mass 12 and the mass 40 region for this channel.

Our article is organized as follows: Section II introduces the formalism of the response functions treated in the RPA. Section III discusses the various final-state channels. In Sec. IV we compare these predictions with the available data. In Sec. V we provide a summary and conclusion of the present work.

II. FORMALISM

The double differential cross section for the reaction $\nu_l(\bar{\nu}_l) + A \longrightarrow l^-(l^+) + X$ is given by

$$\frac{\partial^2\sigma}{\partial\Omega_{k'}\partial k'} = \frac{G_F^2\cos^2\theta_C \boldsymbol{k'}^2}{32\pi^2 k_0 k'_0}|T|^2, \tag{1}$$

where G_F is the weak coupling constant, θ_c the Cabbibo angle, k and k' the initial and final lepton momenta, and T the invariant amplitude given by the contraction of the leptonic L and hadronic W tensors. Their expressions are given in Appendix A. In order to illustrate how the various response functions enter and to introduce the variables, we give below a simplified expression, which in particular ignores the lepton mass contribution and assumes zero Δ width. We stress, however, that in the actual calculations the full formulas of Appendix A, which do not make these simplifications, have been used. The simplified double differential cross section reads

$$\begin{aligned}\frac{\partial^2\sigma}{\partial\Omega\partial k'} = {} & \frac{G_F^2\cos^2\theta_c(\boldsymbol{k}')^2}{2\pi^2}\cos^2\frac{\theta}{2}\left\{G_E^2\left(\frac{q_\mu^2}{\boldsymbol{q}^2}\right)^2 R_\tau^{NN}\right. \\ & + G_A^2\frac{(M_\Delta - M_N)^2}{2\boldsymbol{q}^2}R_{\sigma\tau(L)}^{N\Delta} + G_A^2\frac{(M_\Delta - M_N)^2}{\boldsymbol{q}^2} \\ & \times R_{\sigma\tau(L)}^{\Delta\Delta} + \left(G_M^2\frac{\omega^2}{q^2} + G_A^2\right)\left(-\frac{q_\mu^2}{q^2} + 2\tan^2\frac{\theta}{2}\right) \\ & \times\left[R_{\sigma\tau(T)}^{NN} + 2R_{\sigma\tau(T)}^{N\Delta} + R_{\sigma\tau(T)}^{\Delta\Delta}\right] \pm 2G_A G_M\frac{k+k'}{M_N} \\ & \left.\times\tan^2\frac{\theta}{2}\left[R_{\sigma\tau(T)}^{NN} + 2R_{\sigma\tau(T)}^{N\Delta} + R_{\sigma\tau(T)}^{\Delta\Delta}\right]\right\}\end{aligned} \tag{2}$$

where $q_\mu = k_\mu - k'_\mu = (\omega, q)$ is the four-momentum transferred to the nucleus, θ the scattering angle, M_Δ (M_N) the Δ (nucleon) mass. The electric, magnetic, and axial form factors are taken in the standard dipole parametrization with the following normalizations: $G_E(0) = 1.0$, $G_M(0) = 4.71$, and $G_A(0) = 1.255$. The corresponding cut-off parameters are $M_V = 0.84\,\mathrm{GeV}/c^2$ for the electric and magnetic terms and $M_A = 1.032\,\mathrm{GeV}/c^2$ for the axial one. The plus (minus) sign in Eq. (2) stands for the neutrino (antineutrino) case. A similar expression applies to the process : $\nu_l(\bar{\nu}_l) + A \longrightarrow \nu_l(\bar{\nu}_l) + X$, which involves neutral currents. The various responses R appearing in Eq. (2) are defined according to

$$\begin{aligned}R_\alpha^{PP'} = {} & \sum_n\langle n|\sum_{j=1}^A O_\alpha^P(j)e^{i\boldsymbol{q}\cdot\boldsymbol{x}_j}|0\rangle \\ & \times\langle n|\sum_{k=1}^A O_\alpha^{P'}(k)e^{i\boldsymbol{q}\cdot\boldsymbol{x}_k}|0\rangle^*\delta(\omega - E_n + E_0).\end{aligned} \tag{3}$$

The upper indices (P, P') refer to the type of particle (N or Δ) at the vertices that couples to the external probe. The corresponding operators have the following forms:

$$O_\alpha^N(j) = \tau_j^\pm,\ \ (\boldsymbol{\sigma}_j\cdot\widehat{q})\,\tau_j^\pm,\ \ (\boldsymbol{\sigma}_j\times\widehat{q})^i\tau_j^\pm,$$

for $\alpha = \tau, \sigma\tau(L), \sigma\tau(T)$, and

$$O_\alpha^\Delta(j) = (\boldsymbol{S}_j\cdot\widehat{q})T_j^\pm,\ \ (\boldsymbol{S}_j\times\widehat{q})^i T_j^\pm,$$

for $\alpha = \sigma\tau(L), \sigma\tau(T)$. We have thus defined the inclusive *isospin* (R_τ), *spin-isospin longitudinal* [$R_{\sigma\tau(L)}$], and *spin-isospin transverse* [$R_{\sigma\tau(T)}$] nuclear response functions (the longitudinal and transverse character of these last two responses refers to the direction of the spin operator with respect to the direction of the transferred momentum). The operators S and T are the usual 1/2 to 3/2 transition operators in the spin and isospin space. We have assumed the existence of a scaling law between the nucleon and Δ magnetic and axial form factors [69]:

$$G_M^*/G_M = G_A^*/G_A = f^*/f,$$

where f^* (f) is the $\pi N\Delta$ (πNN) coupling constant. For a matter of convenience, we have incorporated the scaling factor $f^*/f = 2.2$ into the responses.

The presence of the spin-isospin longitudinal coupling is a distinct feature of neutrino interaction as compared to inelastic electron scattering. For instance, coherent pion production present in ν interactions is partly suppressed in (e, e') scattering due to the purely transverse spin coupling of the exchanged photon. Inclusive electron scattering is nevertheless useful as a test for the transverse response [64]. The response functions are related to the imaginary part of the corresponding full polarization propagators

$$R(\omega, q) = -\frac{\mathcal{V}}{\pi}\mathrm{Im}[\Pi(\omega, q, q)], \tag{4}$$

where $\mathcal{V}$ is the nuclear volume such that $\mathcal{V}\rho = A$. They are calculated within a RPA (random phase) ring approximation starting from "bare" propagators (meaning that the nuclear correlations are switched off). The word bare here does not imply that the corresponding response is free of many-body effects, as described in the following. The "bare" polarization propagator is illustrated by some of its components in Fig. 1 where the wiggled lines represent the external probe, the full lines correspond to the propagation of a nucleon (or a hole), the double lines to the propagation of a Δ and the dashed lines to an effective interaction between nucleons and/or Δs.

The dotted lines in Fig. 1 indicate, in each of the channels introduced previously (NN, $N\Delta$, or $\Delta\Delta$), which intermediate state is placed on-shell. It follows that the bare response is the sum of the following partial components: NN: quasielastic (as described by the standard Lindhard function); NN: 2p-2h; $N\Delta$ and ΔN: 2p-2h; $\Delta\Delta$: πN; $\Delta\Delta$: 2p-2h; $\Delta\Delta$: 3p-3h. Notice that the graphs shown in Fig. 1 do not exhaust all the possibilities for the bare propagator. For instance, the distortion of the pion emitted by the Δ is not explicitly shown, although it will be included in our evaluation through the modification of the Δ width in the nuclear medium. But the type of final states that we consider is limited to the previous list. Thus, in the bare case, through the introduction of the partial polarization propagators illustrated by the Feynman graphs of Fig. 1, the inclusive expression of Eq. (2) provides an access to the exclusive ones, with specific final states.

For the actual evaluation of the bare response, i.e., the imaginary piece of the bare propagator, some of the graphs

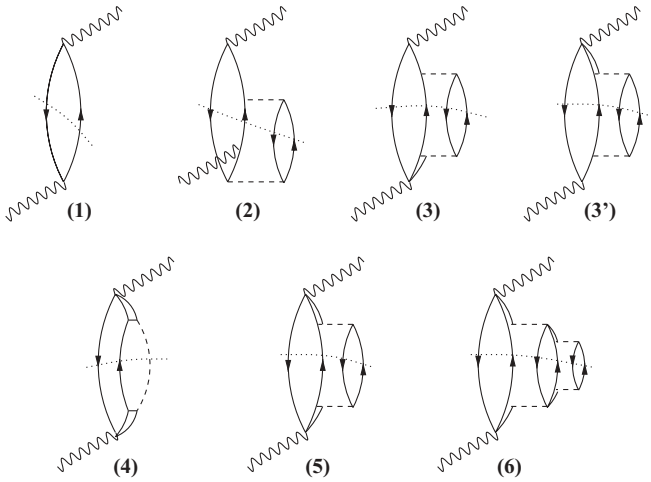

FIG. 1. Feynman graphs of the partial polarization propagators: NN quasielastic (1), NN (2p-2h) (2), $N\Delta$ (2p-2h) (3), ΔN (2p-2h) (3′), $\Delta\Delta$ (πN) (4), $\Delta\Delta$ (2p-2h) (5), $\Delta\Delta$ (3p-3h) (6). The wiggled lines represent the external probe, the full lines correspond to the propagation of a nucleon (or a hole), the double lines to the propagation of a Δ and the dashed lines to an effective interaction between nucleons and/or Δs. The dotted lines show which particles are placed on-shell.

of Fig. 1 amount to a modification of the Δ width in the medium. We take into account this modification through the parametrization of the in-medium Δ width of Oset and Salcedo [70], which leads to a good description of pion-nuclear reactions. The authors split the Δ width into different decay channel contributions: the $\Delta \longrightarrow \pi N$, which is modified by the Pauli blocking of the nucleon and the distortion of the pion. Moreover, in the nuclear medium, new decay channels are possible: the two-body (2p-2h) and three-body (3p-3h) absorption channels that they also incorporate. They give a parametrization for the inclusion of these effects, both in the case of pion interaction with nuclei and for the photoproduction process. We have used their parametrization in spite of the fact that in neutrino interaction the intermediate boson has a spacelike character. An explicit evaluation of the corresponding contributions in the kinematical situation of neutrino scattering is desirable. There exist also other 2p-2h contributions that are not reducible to a modification of the Δ width. We include them, as in the work of Marteau [38], following the method of Delorme and Guichon [71] who perform an extrapolation of the calculations of Ref. [72] on the 2p-2h absorption of pions at threshold. For the last contribution only the imaginary part of the corresponding propagator is incorporated. The explicit expressions are given in Appendix B1. It turns out that for neutrino interaction it is the dominant contribution to the 2p-2h final-state channel, as will be illustrated later. This piece of the cross section is subject to some uncertainty as this parametrization has not been constrained by specific experimental tests. This point will be discussed in more detail in Secs. III C and IV C.

The "bare" polarization propagator is density dependent. In a finite system, $\Pi^0(\omega, \mathbf{q}, \mathbf{q}')$, it is nondiagonal in momentum space. In order to account for the finite size effects we evaluate it in a semiclassical approximation where it can be cast in the

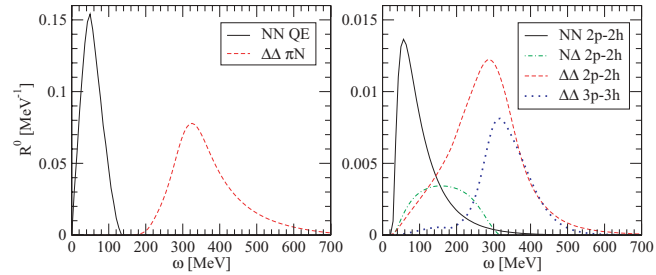

FIG. 2. (Color online) Bare response for ^{12}C at $q = 300$ MeV/c as a function of the energy transfer with its different components, quasielastic and pion emission (left panel), 2p-2h and 3p-3h (right panel).

form

$$\Pi^0(\omega, \boldsymbol{q}, \boldsymbol{q}') = \int d\boldsymbol{r} e^{-i(\boldsymbol{q}-\boldsymbol{q}')\cdot\boldsymbol{r}} \Pi^0\left[\omega, \frac{1}{2}(\boldsymbol{q}+\boldsymbol{q}'), r\right]. \quad (5)$$

In practice we use a local density approximation,

$$\Pi^0\left(\omega, \frac{\boldsymbol{q}+\boldsymbol{q}'}{2}, r\right) = \Pi^0_{k_F(r)}\left(\omega, \frac{q+q'}{2}\right), \quad (6)$$

where the local Fermi momentum $k_F(r)$ is related to the experimental nuclear density through: $k_F(r) = [3/2\pi^2\rho(r)]^{1/3}$. The density profiles of the various nuclei considered are taken from the sum-of-Gaussians nuclear charge density distribution parameters according to Ref. [73]. The corresponding bare response for ^{12}C at $q = 300$ MeV/c as a function of the energy transfer is illustrated in Fig. 2 with its different components, quasielastic, pion emission, 2p-2h and 3p-3h. In all figures the responses incorporate the multiplicative spin-isospin factor.

Turning to the RPA, as the semiclassical approximation is not suited to evaluate the collective effects, we have used the previous bare polarization propagator Π^0 as an input in a full quantum mechanical resolution of the RPA equations in the ring approximation. The introduction of the RPA correlations amounts to solving integral equations that have the generic form:

$$\Pi = \Pi^0 + \Pi^0 V \Pi, \quad (7)$$

where V denotes the effective interaction between *particle-hole* excitations. Its diagrammatic representation is given in Fig. 3. Some detailed expressions are given in Appendix B2.

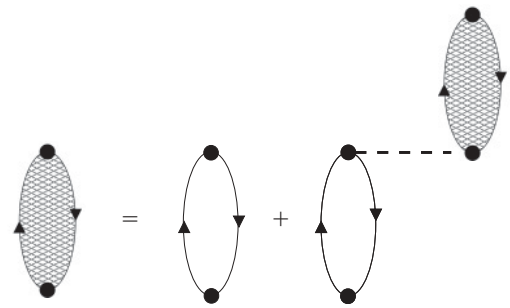

FIG. 3. Diagrammatic representation of the RPA polarization propagator. The white bubble is the free p-h propagator while the black is the full RPA one.

In the spin-isospin channel the RPA equations couple the L and T or the N and Δ components of the polarization propagators. The effective interaction relevant in the isospin and spin-isospin channels is the crucial ingredient for determining the importance of the RPA effects. We use the parametrization in terms of π, ρ and contact pieces:

$$\begin{aligned} V_{NN} &= (f' + V_\pi + V_\rho + V_{g'})\boldsymbol{\tau}_1 \cdot \boldsymbol{\tau}_2 \\ V_{N\Delta} &= (V_\pi + V_\rho + V_{g'})\boldsymbol{\tau}_1 \cdot \boldsymbol{T}_2^\dagger \\ V_{\Delta N} &= (V_\pi + V_\rho + V_{g'})\boldsymbol{T}_1 \cdot \boldsymbol{\tau}_2 \\ V_{\Delta\Delta} &= (V_\pi + V_\rho + V_{g'})\boldsymbol{T}_1 \cdot \boldsymbol{T}_2^\dagger. \end{aligned} \tag{8}$$

For instance, in the NN case one has:

$$\begin{aligned} V_\pi &= \left(\frac{g_r}{2M_N}\right)^2 F_\pi^2 \frac{\boldsymbol{q}^2}{\omega^2 - \boldsymbol{q}^2 - m_\pi^2} \boldsymbol{\sigma}_1 \cdot \widehat{q} \boldsymbol{\sigma}_2 \cdot \widehat{q} \\ V_\rho &= \left(\frac{g_r}{2M_N}\right)^2 C_\rho F_\rho^2 \frac{\boldsymbol{q}^2}{\omega^2 - \boldsymbol{q}^2 - m_\rho^2} \boldsymbol{\sigma}_1 \times \widehat{q} \boldsymbol{\sigma}_2 \times \widehat{q} \\ V_{g'} &= \left(\frac{g_r}{2M_N}\right)^2 F_\pi^2 g' \boldsymbol{\sigma}_1 \cdot \boldsymbol{\sigma}_2, \end{aligned} \tag{9}$$

where g' is the Landau-Migdal parameter and $C_\rho = 1.5$. Here $F_\pi(q) = (\Lambda_\pi^2 - m_\pi^2)/(\Lambda_\pi^2 - q^2)$ and $F_\rho(q) = (\Lambda_\rho^2 - m_\rho^2)/(\Lambda_\rho^2 - q^2)$ are the pion-nucleon and ρ-nucleon form factors, with $\Lambda_\pi = 1$ GeV and $\Lambda_\rho = 1.5$ GeV. For the Landau-Migdal parameter f', we take $f' = 0.6$. As for the spin-isospin parameters g' we use the information of the spin-isospin phenomenology [74], with a consensus for a larger value of $g'_{NN} = 0.7$; for the other parameters we take $g'_{N\Delta} = g'_{\Delta\Delta} = 0.5$.

The separation between the specific channels is less straightforward in the RPA case than in the bare one. Indications can be obtained with the following method, introduced in Ref. [38]. The imaginary part of Π can be written (again generically) as:

$$\mathrm{Im}\Pi = |\Pi|^2 \,\mathrm{Im}V + |1 + \Pi V|^2 \,\mathrm{Im}\Pi^0. \tag{10}$$

It separates into two terms. The first term on the right-hand side of Eq. (10), $|\Pi|^2 \mathrm{Im}V$, is absent when the effective interaction is switched off. In the domain of energy considered it is the imaginary part of the pion exchange potential V_π that plays the major role. This process thus represents the coherent pion production, i.e., the emission of an on-shell pion, the nucleus remaining in its ground state. This is illustrated in Fig. 4, in which the hatched rings represents the RPA polarization propagator. The second term on the right-hand side of Eq. (10), proportional to the bare polarization propagator $\mathrm{Im}\Pi^0$, reflects the type of final state already mentioned for the imaginary part of Π_0: $NN, \pi N, \ldots$. The factor in front, $|1 + \Pi V|^2$, embodies the modification of the exclusive bare responses by the collective effects. We point out, however, that final-state interactions are not incorporated in this description. For instance, a pion produced in the decay of the Δ resonance can be absorbed on its way out leading to a multinucleon emission process. Thus the second term in Eq. (10) is adequate for the sum of the incoherent pion production and the multinucleon knock-out channels but not for each channel individually.

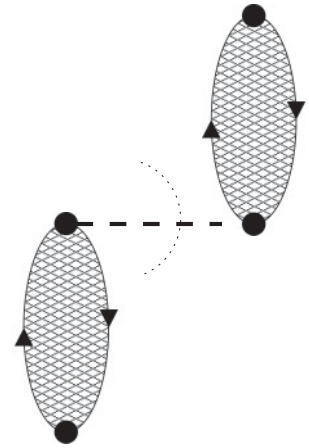

FIG. 4. Diagrammatic representation of the coherent process. The dotted line indicates that pion is placed on-shell.

The separation between these two channels from the type of final state is approximate for light nuclei such as ^{12}C. In heavier nuclei it overestimates the incoherent pion channel, underestimating the multinucleon one. We will illustrate this fact in the scattering of physical pions.

Having established the formalism, we are now ready to evaluate the cross sections in the various partial channels. In the actual numerical calculation we have limited the energy transfer to $\omega = 1$ GeV as our approach becomes insufficient for a larger energy transfer. The center-of-mass correction for the π-N system $q_{\mathrm{CM}} = \frac{q}{1+\omega/M}$ [75] is made by dividing the bare responses by a factor $r^2 = (1 + \omega/M)^2$. The components of the neutrino cross section that does not involve the momentum q at the two ends of the RPA chain are obtained by an overall multiplication by the factor r^2. Interference terms with one momentum are multiplied by r.

III. RESULTS

A. Coherent cross section

Several types of responses enter the total neutrino cross section, isovector, spin-isospin: transverse or longitudinal. The last quantity is naturally associated with the coherent process, because it has the same coupling as the pion. The production by a transverse spin coupling requires a transverse-longitudinal conversion that is partly suppressed. This difference is illustrated in Fig. 5 where the total responses, longitudinal and transverse, of ^{12}C are displayed as a function of the energy transferred to the nuclear system for a fixed three-momentum $q = 300\,\mathrm{MeV}/c$. The coherent component, much larger in the longitudinal case, is also shown.

Figure 6 illustrates the evolution with the nuclear size of the coherent part of the longitudinal response *per nucleon* as a function of the energy at fixed momentum for some nuclei, ^{12}C, ^{16}O, ^{40}Ca, and also for a fictitious piece of isospin symmetric nuclear matter with the density profile of lead. Two features emerge, the first one is that its magnitude decreases in "lead," as expected: the coherent response per nucleon vanishes in nuclear matter when the polarization propagators become diagonal in momentum space. The second is that the coherent

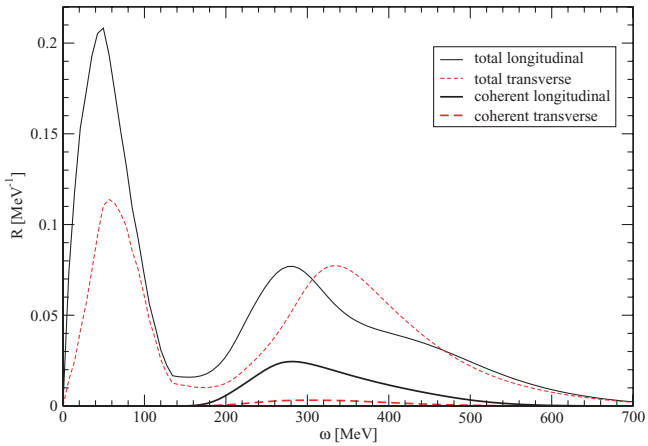

FIG. 5. (Color online) Longitudinal and transverse total responses of ^{12}C at fixed $q = 300\,\mathrm{MeV}/c$ as a function of ω. The coherent part of the responses is also shown.

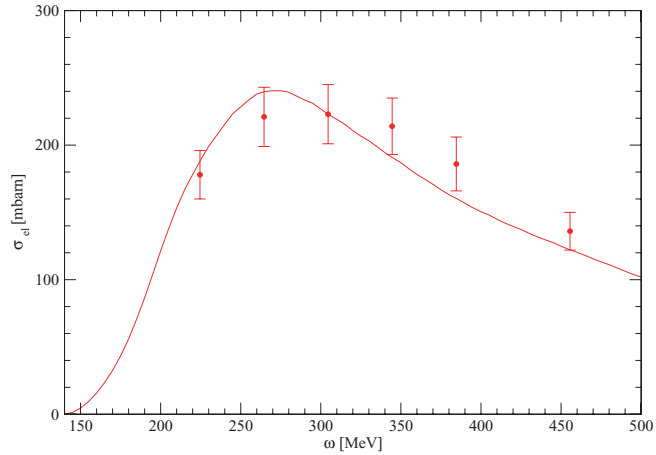

FIG. 7. (Color online) π-^{12}C elastic cross section as a function of pion energy.

response is not peaked at the energy $\omega_\pi = (q^2 + m_\pi^2)^{1/2}$ where the mismatch between the incident energy and that of the physical outgoing pion is smallest. Instead, it is reshaped by the collective features of the longitudinal response with the appearance of two collective branches on each side of the pion line. This is more apparent in the case of the (fictitious) lead.

As a test of our description of the coherent responses we have investigated the elastic scattering of pions on nuclei in the Δ region, related to the coherent part of the spin-isospin longitudinal response through:

$$\sigma^{\mathrm{elas}}(\omega) = \left(\frac{g_r}{2M_N}\right)^2 \pi q_\pi R_L^{\mathrm{coh}}(\omega, q_\pi), \qquad (11)$$

where $q_\pi^2 = \omega^2 - m_\pi^2$ and R_L^{coh} refers to the coherent part of the longitudinal response. The resulting cross-section in the case of ^{12}C is shown in Fig. 7 together with the experimental points from Ref. [76]. The agreement with data is satisfactory. A similar accuracy can be expected for the coherent response that enters the neutrino cross section, at least in the energy region for the produced pion where we have tested our model (i.e., between $\omega \simeq 220$ and $\simeq$450 MeV). The elastic cross section that depends on the longitudinal response is particularly sensitive to collective effects in this channel known to be important. The replacement of the bare response by the RPA one leads to a different energy behavior, the collective effects producing a softening of the response, characteristic of the collective nature of the longitudinal channel.

Figure 8 displays our evaluations of the neutrino coherent cross section on ^{12}C as a function of the pion kinetic energy, both for charged and neutral current, for several neutrino incident energies. The resulting total coherent cross sections are displayed in Fig. 9. The suppression of the meson exchange correction in the time component of the axial current, $G_A^* \to G_A$, produces a moderate $\simeq$10% increase of the cross section.

The data available on the coherent production by neutrino concern its ratio to the total cross section and to the total pion production. We will then postpone the comparison with experimental data after the discussion of the various other channels.

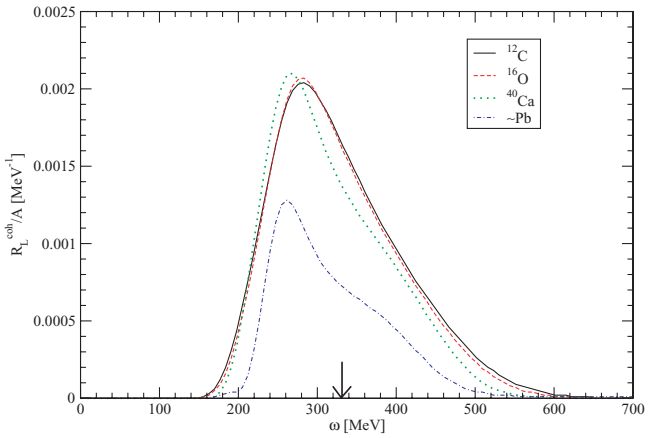

FIG. 6. (Color online) Evolution with the mass number of the coherent longitudinal response per nucleon at fixed $q = 300\,\mathrm{MeV}/c$ as a function of ω. The arrow indicates the energy for on-shell pion.

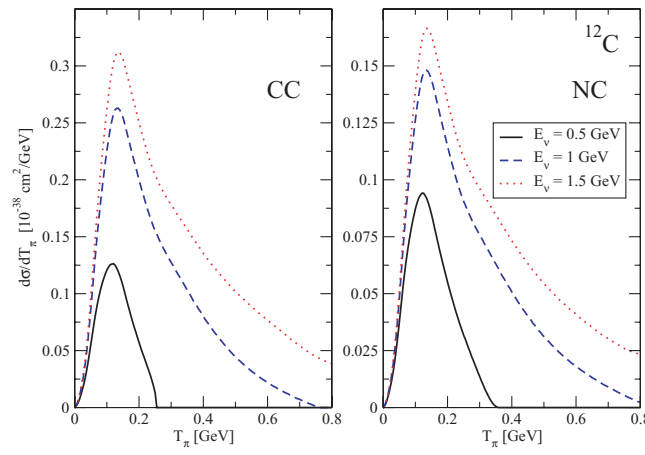

FIG. 8. (Color online) Charged and neutral current coherent pion production differential cross section off ^{12}C versus pion kinetic energy for several ν_μ energies.

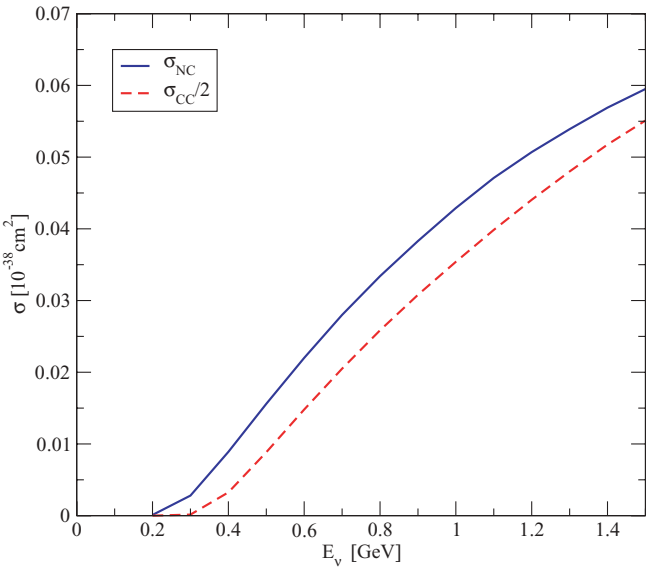

FIG. 9. (Color online) Total CC (divided by 2) and NC ν_μ-induced coherent pion production cross sections in ^{12}C as a function of neutrino energy.

1. Adler's theorem

In the forward direction where $q = \omega$ and for vanishing lepton mass, only the spin longitudinal response contribution survives. As it also enters in pion scattering, it is possible to relate the forward neutrino cross section to the cross section of physical pions, apart from a difference in kinematics: $q = \omega$ (soft pions) for neutrinos, instead of $q = q_\pi = \sqrt{\omega^2 - m_\pi^2}$ for physical pions. This difference becomes less relevant at large energies. This is the content of Adler's theorem [77]. The coherent channel, which is completely dominated by the longitudinal response, offers the best application of this theorem, while for the other channels the transverse component, which bears no relation to pion scattering, quickly takes over as soon as one moves away from the forward direction. This theorem has been used in the approach of Refs. [18,29,31] to evaluate the coherent neutrino-nucleus cross section. This is not our aim here. We want to illustrate the link between the forward direction coherent neutrino cross section and the elastic pion-nucleus one. For the coherent cross section Adler's relation writes

$$\left(\frac{\partial^2\sigma}{\partial\Omega\partial\omega}\right)^{\rm coh}_{\theta=0} = \frac{G_F^2\cos^2\theta_c}{\pi^3} f_\pi^2 \frac{(E_\nu-\omega)^2}{\omega}\sigma^{\rm elas}(\omega), \quad (12)$$

where $f_\pi = 93.2\,$MeV is the neutral pion decay constant. Introducing the experimental values for the elastic cross section taken from Ref. [76] we obtain the points shown in Fig. 10 together with our predicted curve. The agreement is rather good. It deteriorates at small energies when the kinematical difference between soft and physical pions becomes substantial. A natural correction can be performed with the introduction into the right-hand side of Eq. (12) of a multiplicative factor $\frac{\omega}{q_\pi}$ as suggested by the relation of Eq. (11) between R_L and $\sigma^{\rm elas}$. The corresponding corrected points are also shown in Fig. 10 extending somewhat the region of agreement. The use of the Adler relation becomes

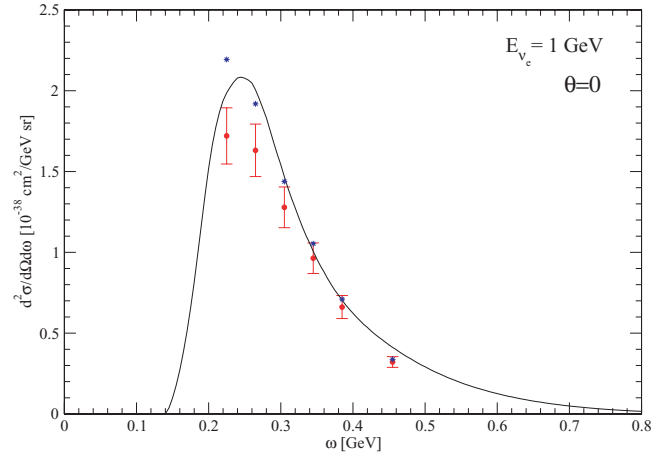

FIG. 10. (Color online) ν_e-^{12}C coherent cross section in the forward direction. (Continuous line) Our result. (Circles) Deduced, according to Adler's relation of Eq. (12), from the experimental values for the elastic cross section taken from Ref. [76]. (Stars) Introducing into the right-hand side of Eq. (12) the multiplicative factor $\frac{\omega}{q_\pi}$.

problematic at energies near threshold. For small neutrino energy ($E_\nu < 0.5\,$GeV) this region has more weight in the total coherent cross section.

The Adler relation thus provides a good test for our evaluation of coherent neutrino cross section in the forward direction. We believe that the extrapolation to the nonforward direction as performed in our model should be under control.

B. Pion-nucleus cross sections

The various partial cross sections for physical pions on nuclei constitute a precious piece of information. Elastic cross section has already been introduced as a test for the coherent cross section. The total cross section for pions on the nuclei is given by an expression similar to Eq. (11) with the full polarization propagator replacing the coherent piece

$$\sigma^{\rm tot}(\omega) = \left(\frac{g_r}{2M_N}\right)^2 \pi q_\pi R_L(\omega, q_\pi). \quad (13)$$

The corresponding cross section is displayed in Fig. 11 together with the experimental points. We will show that in the same way the inelastic cross section provides some information on the incoherent pion production by neutrinos and the absorptive cross section on the multinucleon channels. Figure 11 displays the various partial channels (but the elastic one, previously shown) that contribute to the π^+ cross section on ^{12}C, namely the inelastic pion scattering channel (which is the incoherent scattering with a π^+ in the final state) and the absorptive one. We also display the sum of the incoherent pion (including charge exchange) and true absorption (multinucleon channels) cross sections. The experimental points are taken from Ashery *et al.* [76]. To reduce the clutter, we have not explicitly plotted the charge-exchange cross section that, in our approach, is one-fifth of the inelastic π^+ cross section and is consistent with the experimental data. While the elastic cross section was well reproduced, our approach

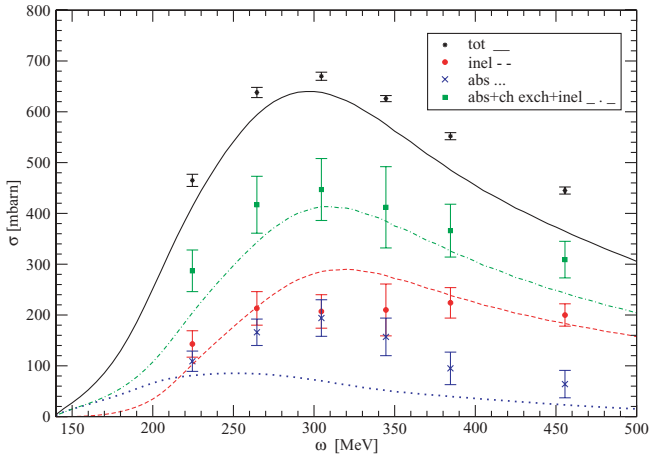

FIG. 11. (Color online) Partial and total π-^{12}C cross sections.

overestimates the π^+ inelastic channel in the peak region and largely underestimates the absorptive channel. We attribute this deficiency to the absence of pion final-state interaction as the pion can be reabsorbed on its way out the nucleus. It can also undergo charge exchange process but this is a smaller effect. As a counterpart the absorptive multinucleon production is underestimated, as is apparent in Fig. 11. The sum of the two channels is instead reasonably well reproduced in the peak region.

These limitations also affect the incoherent neutrino-nucleus cross section but we stress that, in contradistinction, our description for the coherent channel automatically contains the final-state interactions and no further correction is needed. The total neutrino cross section is also obviously not affected. With the information on the pion energy spectrum in neutrino interactions (that our calculation does not provide) it would be possible to estimate at each energy an attenuation factor for the incoherent neutrino production from the difference between our calculation and inelastic data for physical pions. For instance, for ^{12}C at $E_\nu = 1$ GeV, a rough evaluation of the overall correction for the incoherent production cross section with the information on the pion spectrum [78] results in a moderate reduction of $\simeq$15%. A similar attenuation was found in oxygen at $E_\nu = 500$ MeV and $E_\nu = 750$ MeV [43]. A larger correction is obviously expected for calcium.

C. Quasielastic and multinucleon channels

The quasielastic (QE) channel corresponds to a single nucleon knock-out. In the quasielastic process the spacelike character is pronounced as the quasielastic peak occurs at $\omega \simeq \mathbf{q}^2/(2M_N)$, hence the distribution in $Q^2 = \mathbf{q}^2 - \omega^2$ is rather broad [9]. At zero order only R^{NN} contributes to this channel. In the RPA chain instead $R^{N\Delta}$ and $R^{\Delta\Delta}$ also participate. For instance, the lowest-order contribution of $R^{N\Delta}$ is illustrated in Fig. 12. In contrast to the coherent channel, the quasielastic one is totally dominated by the transverse response. The longitudinal contribution is suppressed by a cancellation between the space and time components of the axial current, as observed by Marteau [38] and shown in

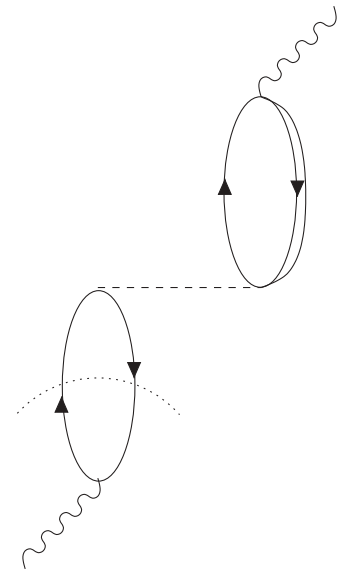

FIG. 12. Lowest-order contribution of $R^{N\Delta}$ to the quasielastic channel.

Appendix A1 for vanishing lepton mass and neglecting the Fermi momentum. Numerically its contribution is indeed very small. We have tested our semiclassical approximation on the bare QE ν_e-^{12}C cross section through a comparison with the one obtained by Martini *et al.* [53] in the continuum shell model where the mean field is produced by a Woods-Saxon well. Our result is very similar in shape and magnitude to the one of Ref. [53] but for a displacement in energy of 27 MeV. This reflects the inclusion of the nucleon separation energy in the continuum shell model, which is ignored in our approximation.

The quasielastic cross section is displayed in Fig. 13 as a function of the energy transfer for neutrino energy $E_\nu = 1$ GeV, both in the bare case and in the RPA one. The RPA influence produces a reduction, as expected from the repulsive character of the particle-hole interaction, which prevails in the transverse channel. This reduction is mostly due to the

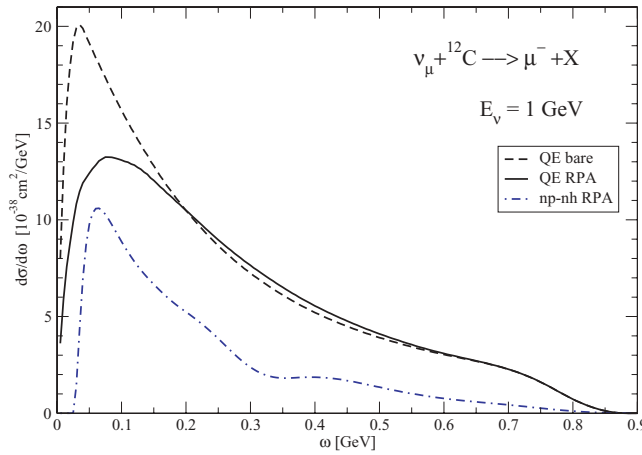

FIG. 13. (Color online) Differential CC ν_μ-^{12}C cross section versus the energy transfer for quasielastic process (bare and RPA) and multinucleon emission (np-nh).

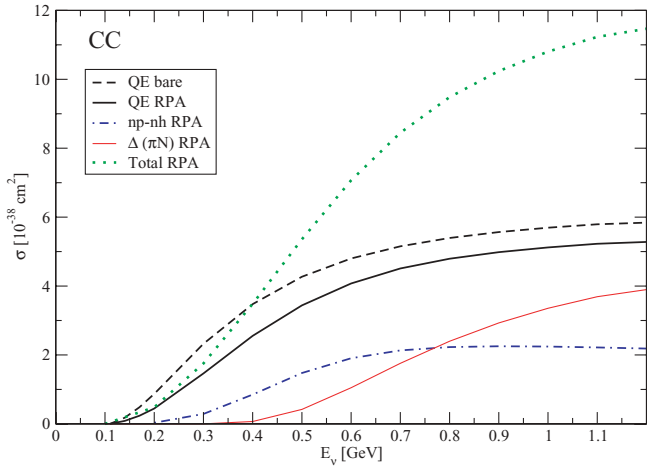

FIG. 14. (Color online) CC ν_μ-^{12}C QE, multinucleon (np-nh), incoherent pion emission, and total cross section as a function of neutrino energy.

interference term $R^{N\Delta}$ that is negative (Lorentz-Lorenz effect [79]).

The total quasielastic charged current and neutral current cross section are plotted in Figs. 14 and 15 as a function of the neutrino energy. In Figs. 13, 14, and 15 we also display the sum of the two- and three-nucleon knock-out cross sections, which represents a sizable fraction of the quasielastic one. Singling out the genuine quasielastic process requires the insurance that no more than one proton is ejected. This question will appear in the comparison with data. Among the various contributions to the multinucleon channel the ones that do not reduce to a modification of the Δ width are dominant. The accumulation of 2p-2h strength at low energy is an artifact of the simplified extrapolation that we use in this channel. In Sec. IV C this point is discussed in more detail and another method for the parametrization, with an explicit momentum dependence, is introduced. It modifies the ω dependence of $\frac{d\sigma}{d\omega}$, spreading the

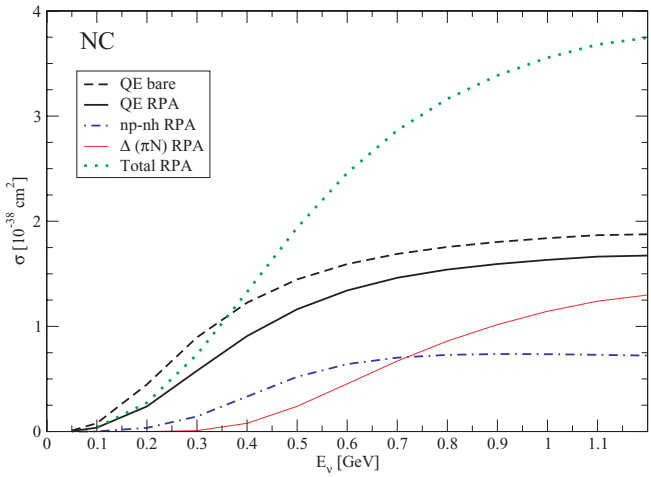

FIG. 15. (Color online) NC ν_μ-^{12}C QE, multinucleon (np-nh), incoherent pion emission, and total cross section as a function of neutrino energy.

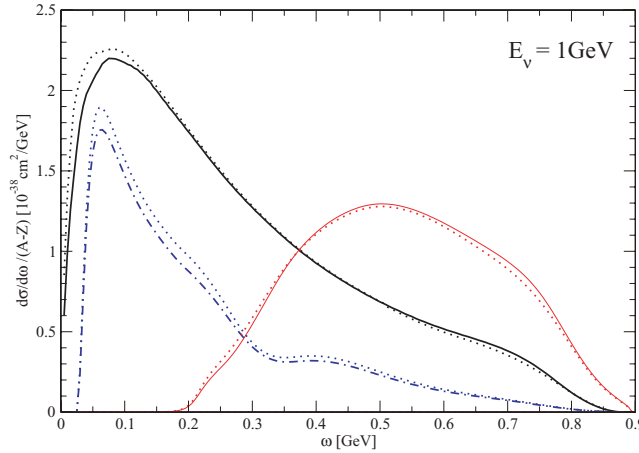

FIG. 16. (Color online) RPA differential CC cross sections per neutron in the different channels for ^{12}C (same convention line as Figs. 13, 14, 15) and ^{40}Ca (dotted lines).

strength over a larger energy region but does not substantially affect the energy integrated cross section.

Coming now to the evolution of these channels between ^{12}C and ^{40}Ca we compare the corresponding RPA differential cross sections per neutron for the two nuclei in Fig. 16. One can see that the evolution of this quantity with the mass number is quite weak in the QE case. It is also weak in the multinucleon channel although it should increase faster with density than the quasielastic one. However, between a light system such as ^{12}C and ^{40}Ca the evolution is moderate. Only in the case of deuteron one expects the multinucleon knock-out to be appreciably smaller in view of the loose binding of the system.

D. Incoherent pion emission

The pion arises from the pionic decay of the Δ leaving the nucleus in a p-h excited state. For the nuclei that we consider this cross section is much larger than the coherent one. As compared to a free nucleon the emission probability is already appreciably reduced in the bare case by the change in the Δ width. Moreover the RPA effects, which are moderate, also tend to a small reduction. The reduction due to the modification of the Δ width has a counterpart in the presence of a component of multinucleon knock-out. Charged current and neutral current cross sections for incoherent pion emission for all possibles charges are represented in Fig. 14 and 15 as a function of neutrino energy. Moreover these figures summarize all previous results for the other channels and also give the total cross sections.

On the other hand, Fig. 16 compares the neutrino differential cross section per neutron in the various channels as a function of the energy transfer, ω, for the cases of ^{12}C and ^{40}Ca and for a neutrino energy $E_\nu = 1$ GeV. The two sets of curves are very similar. We can conclude that, at the level of our approximation, i.e., without final-state interaction, it is possible to extrapolate smoothly from ^{12}C to the region of ^{40}Ar. Only the coherent cross section presents a significant variation, illustrated in Fig. 17.

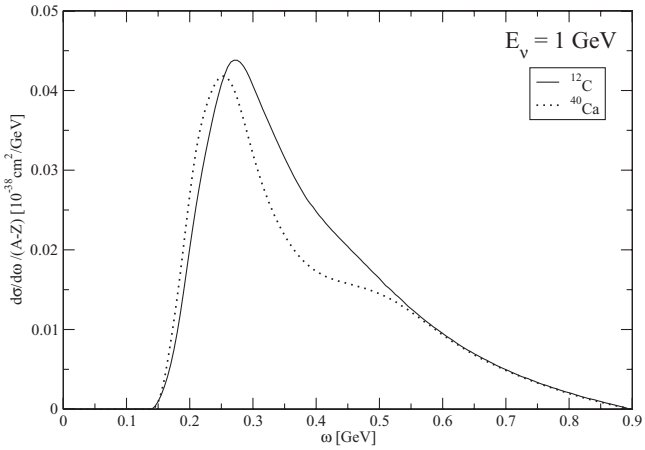

FIG. 17. Differential CC cross sections per neutron in the coherent channel for ^{12}C (continuous line) and ^{40}Ca (dotted line).

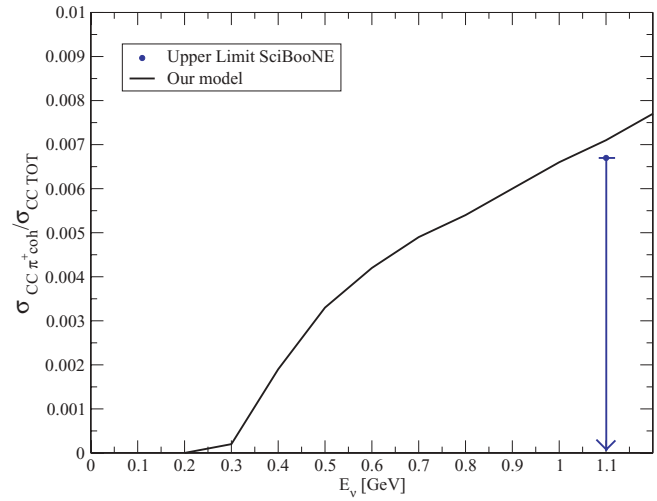

FIG. 18. (Color online) Ratio of the ν_μ-induced charged current coherent π^+ production to total cross section as a function of neutrino energy.

IV. COMPARISON WITH DATA

A. Coherent pion production

Experimental data concern ratios between different cross sections. The first indication of coherent pion production by neutral current was given by MiniBooNE [10], which found the ratio of coherent to total π^0 production to be $0.195 \pm 0.011 \pm 0.025$. In this experiment the neutrino flux is spread in energy with a peak at $\simeq$700 MeV [13]. Our approach leads to a lower number, namely 0.06, which is difficult to reconcile with experimental data, a problem that other groups also face. It has been suggested in Ref. [27] that MiniBooNE, which uses Rein-Sehgal model [80] for data analysis, possibly overestimates the π^0 coherent cross section. In a preliminary report [81] the experimental value given for this cross section is $(7.7 \pm 1.6 \pm 3.6) \times 10^{-40}$ cm^2. Our result for this cross section averaged on the MiniBooNE flux [13], 2.8×10^{-40} cm^2, is compatible with the experiment in view of the large experimental errors.

On the other hand, for charged current, two experimental groups have given upper limits for the ratio of coherent pion production to the total cross section. The K2K collaboration gives a limit of 0.6010^{-2} averaged over a neutrino flux with a mean energy of 1.3 GeV [7]. More recently, the SciBooNE collaboration found for the same quantity 0.6710^{-2} at neutrino energy of 1.1 GeV [12] and 1.3610^{-2} at neutrino energy of 2.2 GeV. We report in Fig. 18 our prediction for this quantity. Because our approach is appropriate for a limited neutrino energy range we keep in the comparison only the lowest energy SciBooNE point. Our curve is just compatible with the experimental bound.

B. Total pion production

Another measured quantity is the ratio of π^+ production to quasielastic cross section for charged current. The MiniBooNE collaboration has used a CH_2 target. In order to compare with ANL [82] and K2K [11] data, they presented the results with an isoscalar rescaling correction [14]. The issue of pion loss by final-state interaction, which is not incorporated in our description, has also been taken into account by MiniBooNE, who correct data for this effect. We can thus compare our π^+ over quasielastic ratio (solid line in Fig. 19) to the final-state-interaction-corrected MiniBooNE results. Our curve incorporates the small coherent cross section; the incoherent pion one is multiplied by the isospin factor 5/6 to single out π^+ contribution. Our curve is fully compatible with experimental data.

As an additional information, MiniBooNE also gives a ratio more directly related to the measurements, namely the ratio of pionlike events (defined as events with exactly one μ^- and one π^+ escaping the struck nucleus) and quasielastic signal (defined as those with one μ^- and no pions). In our language the last quantity represents the total Np-Nh ($N = 1, 2, 3$, including the quasielastic for $N = 1$) exclusive channel. We have compared this second experimental information to the ratio between our calculated pion production (which, however, ignores final-state interactions) and our total Np-Nh contribution to the total charged current neutrino cross section (Fig. 20). There is an appreciable difference between the

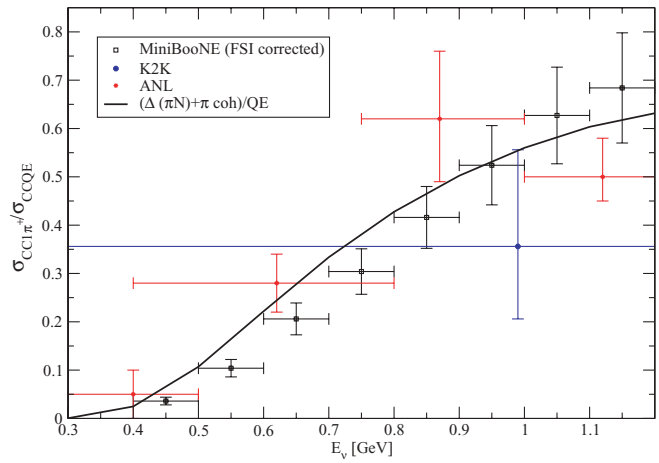

FIG. 19. (Color online) Ratio of the ν_μ-induced charged current one π^+ production to quasielastic cross section as a function of neutrino energy. The final-state-interaction-corrected data are taken from Ref. [14].

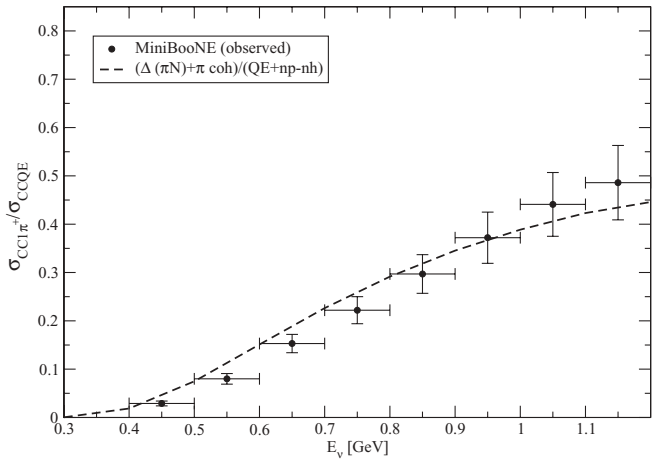

FIG. 20. Ratio of the ν_μ-induced charged current one π^+ production to quasi-elastic-like cross section as a function of neutrino energy. The "observed" data are taken from Ref. [14].

two curves of Fig. 19 and Fig. 20: the one of Fig. 20 is reduced due to a large 2p-2h component in the Np-Nh cross section, which increases the denominator. The comparison with the experiment shows an agreement up to $E_\nu \simeq 1.2$ GeV. Final-state interactions for the pion, which are not included, are expected to reduce our result at the level of 15%, still maintaining an agreement.

A new result has been presented at NuInt09 by SciBooNE [16]. It is the ratio of the total neutral current π^0 production cross section to the total charged current cross section at the mean neutrino neutrino energy of 1.16 GeV. They obtain the preliminary value:

$$\frac{\sigma(\mathrm{NC}\pi_0)}{\sigma(\mathrm{CC_{TOT}})} = \left[7.7 \pm 0.5(\mathrm{stat.})^{+0.4}_{-0.5}(\mathrm{sys.})\right] \times 10^{-2}. \quad (14)$$

Our prediction for this quantity, including coherent contribution and a factor 2/3 for NC incoherent pion production to single out π^0 contribution is:

$$\frac{\sigma(\mathrm{NC}\pi_0)}{\sigma(\mathrm{CC_{TOT}})} = 7.9 \times 10^{-2}, \quad (15)$$

which fully agrees with data.

A general comment on the comparison with data: nearly all the ratios that have been discussed, except the final-state-interaction-corrected MiniBooNE result of Fig. 19, are sensitive to the presence of the np-nh ($n = 2, 3$) component in the cross section. Because the size magnitude is not so well tested, we can investigate what becomes the comparison with data in the extreme situation when we totally suppress this contribution. For the last ratio discussed we obtain

$$\frac{\sigma(\mathrm{NC}\pi_0)}{[\sigma(\mathrm{CC_{TOT}}) - \sigma(\mathrm{CC}_{np-nh})]} = 9.8 \times 10^{-2}, \quad (16)$$

appreciably above the experimental value.

As for the SciBooNE upper limit of the ratio of the π^+ coherent to total charged current cross section, our prediction at $E_\nu = 1.1$ GeV, which was 0.71×10^{-2}, without np-nh becomes 0.89×10^{-2}, further above the experimental bound of 0.67×10^{-2}.

C. Quasielastic cross section

A new preliminary result on absolute cross sections has been presented by the MiniBooNE collaboration [15]. This group gives in particular the absolute value of the cross section for "quasielastic" events, averaged over the neutrino flux and as a function of neutrino energy. The comparison of these results with a prediction based on the relativistic Fermi gas model using the standard value of the axial cut-off mass $M_A = 1.03\,\mathrm{GeV}/c^2$ reveals a substantial discrepancy. In the same model a modification of the axial cut-off mass from the standard value to the larger value $M_A = 1.35\,\mathrm{GeV}/c^2$ is needed to account for data. A similar conclusion holds for the Q^2 distribution [8,9]. The introduction of a realistic spectral function for the nucleon does not alter this conclusion [32].

As a possible interpretation we question here the real definition of quasielastic events. As already discussed above, the nuclear medium is not a gas of independent nucleons, correlated only by the Pauli principle, but there are additional correlations. The ejection of a single nucleon (denoted as a genuine quasielastic event) is only one possibility, and one must in addition consider events involving a correlated nucleon pair from which the partner nucleon is also ejected. This leads to the excitation of two-particle–two-hole (2p-2h) states that have been abundantly discussed throughout this work. In the spin-isospin channel the correlations, mostly the tensor ones, add 2p-2h strength to the 1p-1h events [66]. At present, in neutrino reactions, such events cannot be experimentally distinguished from the genuine quasielastic events and must be considered simultaneously. Notice that the standard lower value of the axial mass, $M_A = 1.03\,\mathrm{GeV}/c^2$, results from deuterium bubble chamber experiments. In this case the effect of tensor correlation is also present but at a lower level because deuteron is a dilute system. Our sum of the combined ^{12}C quasielastic cross section and the 2p-2h one is displayed in Fig. 21. This prediction fits the experimental data excellently, better than expected in view of the uncertainties of our 2p-2h

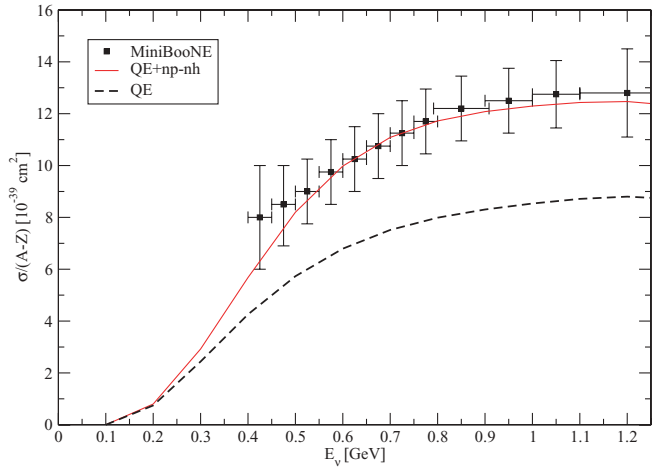

FIG. 21. (Color online) "Quasielastic" ν_μ-^{12}C cross section per neutron as a function of neutrino energy. Dashed curve: pure quasielastic (1p-1h) cross section; solid curve: with the inclusion of np-nh component. The experimental MiniBooNE points are taken from Ref. [15].

cross section. As for the flux averaged "quasielastic" cross section per neutron the experimental value is 9.4×10^{-39} cm^2 (with a normalization error of 11%). Our prediction for this quantity is 6.3×10^{-39} cm^2 without 2p-2h contribution and 9.0×10^{-39} cm^2 including it, a value more in touch with the experimental one.

In view of the importance of the issue we want to investigate if this large 2p-2h contribution is a genuine effect and not an artifact of the particular parametrization that we have used for the bare 2p-2h channel. For this, we introduce a different approach that exploits a microscopic evaluation by Alberico *et al.* [66] of the 2p-2h contribution to the transverse magnetic response of (e, e') scattering. It does not have the shortcomings of our previous parametrizations that have no momentum dependence. In the previous case the maximum of the 2p-2h response $R^{NN}_{\rm 2p-2h}$ always lies at low energy, $\omega \simeq 50$ MeV, irrespective of the momentum, separating at large momentum from the quasielastic peak that instead gets shifted at larger energies. A similar feature exists in the $N\Delta$ part. This is not realistic and below we sketch a possible way for improvements. The aim is to extract the 2p-2h responses from the results of Alberico *et al.* [66], although they are available for a limited set of momenta and energies and they concern iron instead of carbon. We have thus performed extrapolations both to cover all the kinematical region of neutrino reactions and to go to the ^{12}C case. For the set of $R_{\sigma\tau(T)}(\omega, q)$ values that we could extract [66] we have observed an approximate scaling behavior with respect to the variable $x = \frac{q^2-\omega^2}{2M_N\omega}$. A parametrization of the responses in terms of this variable allows the extrapolation needed to cover the full neutrino kinematical region and we have now the new responses, $R^{NN}_{\rm 2p-2h}(\omega, q)$ and $R^{N\Delta}_{\rm 2p-2h}(\omega, q)$ in all the range. For the $\Delta\Delta$ part, which is not well covered in Ref. [66] we have kept the previous parametrization, which already presents a proper q dependence owing to the contribution of the in-medium Δ width [70]. Another remark is in order. The evluation of Ref. [66] of the 2p-2h channel does not reproduce pion absorption in nuclei at threshold, as observed by the authors. It gives a too large value for the absorptive p-wave optical potential parameter [75], $\mathrm{Im}C_0 \simeq 0.18 m_\pi^{-6}$, instead of the best fit value $\mathrm{Im}C_0 \simeq 0.11 m_\pi^{-6}$. To be as consistent as possible with our previous parametrization, which comes from pion absorption, we have applied to our scaling function the reduction factor $\frac{0.11}{0.18}$. The nuclear mass dependence is taken care of with the introduction of the Levinger factor, L, which fixes the number of quasideuteron pairs in the nucleus defined as LZN/A. We rescale the iron results by a factor r, ratio of the Levinger factors, for the two nuclei. It is $r = 0.8$ according to the A dependence of the Laget formula [83] or a similar value, $r \simeq 0.75$ from Ref. [84]. Altogether the global reduction factor applied to the iron scaling function is $\simeq$0.5.

Because in the previous case the RPA have little effect on the 2p-2h component, we introduce directly the bare new 2p-2h quantities in the neutrino cross section. The influence of the new modelization of the 2p-2h is displayed in Fig. 22, where the bare partial and total np-nh differential CC neutrino cross sections at $E_\nu = 0.7$ GeV are shown both for the previous parametrization and for the new one. The energy behaviors are quite different, the NN contribution is no longer localized

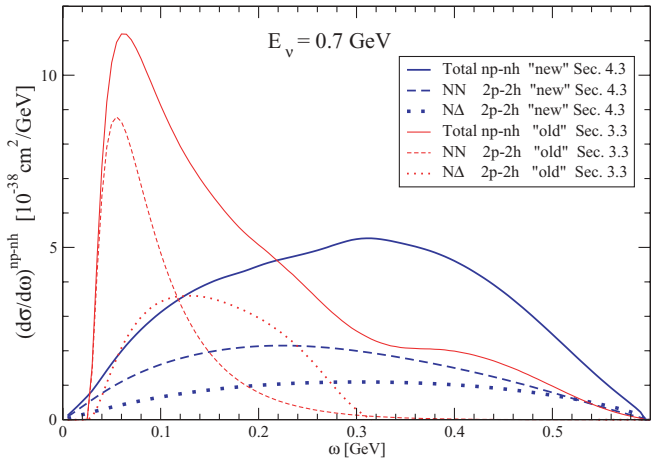

FIG. 22. (Color online) Comparison between the CC ν_μ-^{12}C np-nh ($n = 2, 3$) differential cross sections deduced from the two different parametrizations of the 2p-2h components. (Thin lines) Parametrization of Sec. III C and used throughout the whole article (denoted "old"); (bold lines) parametrization of Sec. IV C ("new").

at small energies but is spread over the whole energy range, a more realistic feature. A similar behavior occurs for $N\Delta$ part. However, the integral over the energy, $\sigma_{n\mathrm{p}-n\mathrm{h}}(E_\nu)$, is practically not modified. As a consequence adding this contributions to the quasielastic cross section we reach a similar conclusion as before about the important role of the multinucleon channel, as illustrated in Fig. 23.

It indicates that, in the nuclear medium, neutrinos in this energy range do not interact only with individual nucleons but also with pairs of nucleons, mostly n-p pairs correlated by the tensor interaction. The spin-dependent part of the neutrino interaction with such a pair is stronger than with the same two nucleons when isolated. This increase manifests itself through the 2p-2h strength that adds to the 1p-1h part, an effect simulated by an increase of the axial cut-off mass. Quantitatively a confirmation on the theoretical side of the exact magnitude through a detailed microscopic calculation of the bare 2p-2h response, which will then be inserted in our RPA formalism, would be helpful. Also an experimental identification of the final state would be of a great importance to clarify this point. In particular the charge of the ejected nucleons will be quite significant. Because tensor correlations involve n-p pairs, the ejected pair is predominantly p-p (n-n) for charged current neutrino (antineutrino) reactions and n-p for neutral current. This predominance has the same origin as

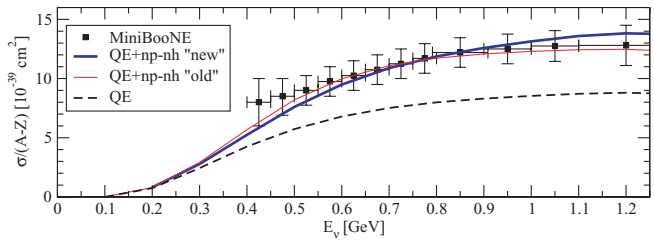

FIG. 23. (Color online) Same as Fig. 21 including also our curve (QE + np-nh "new") with the new parametrization for the 2p-2h component (bold line).

for p-wave π^- absorption by nuclei where n-n emission is favored over n-p emission [72,79].

V. SUMMARY AND CONCLUSION

We have studied neutrino interactions with light nuclei that enter the targets of present or future experiments. Our theoretical tool is the theory of the nuclear response treated in the RPA, a well-established technique for the treatment of electromagnetic or weak interactions with nuclei and that have been used also for strongly interacting probes. The crucial element of the RPA treatment is the p-h interaction, in particular for the spin-isospin one, which has been taken from the accumulated knowledge on the spin-isospin responses. The main merit of this approach is to allow unified description of various channels. It has some limitations that restrict the energy range of the neutrino to a region below $\simeq$1.2 GeV. For instance, the only nucleonic resonance incorporated in the description is the Δ resonance. Multipion production is also ignored, as well as most meson exchange effects. Moreover, although both the Δ propagator and the center-of-mass correction are the relativistic one, not all relativistic effects are included in a systematic way.

The final states considered are the quasielastic, 2p-2h, 3p-3h ones, and coherent or incoherent pion production. Some channels have the problem that final-state interactions are not incorporated. This is the case for incoherent pion emission where the produced pion can be absorbed on its way out of the nucleus leading to a multinucleon state. Incoherent pion production is therefore overestimated and the multinucleon channel accordingly underestimated. This effect is visible in the scattering of physical pions on ^{12}C in the region of the Δ peak. For a light nucleus such as ^{12}C the effect is limited but it becomes more serious in heavier nuclei. Our method should be supplemented by an evaluation of the final-state interaction, for instance, by a Monte Carlo method [61,85].

The coherent channel is particularly interesting, although it represents only a small fraction of the total pion emission. It does not suffer from the previous limitations as final-state interactions are automatically incorporated in the RPA treatment that is particularly suited for this channel. Moreover, it is the only channel that is dominated by the isospin spin-longitudinal response where collective effects are very pronounced while they remain moderate in the other channels. The difference between the first-order term with one bubble (with Δ excitation) and the full RPA chain is quite large. In this context we have used as a test of our spin longitudinal response the experimental data on elastic pion scattering in the Δ region. It offers a direct test of the forward coherent neutrino cross section to which it is linked through the Adler theorem. Except for low pion energies near threshold ($\omega \leqslant 200$ MeV) where Adler's theorem fails, the elastic cross section can be used to extract the forward neutrino coherent cross section as in the method of Rein-Sehgal.

For the evolution of the partial cross sections with mass number in order to reach the ^{40}Ca region, our description indicates that, apart from the coherent pion production that evolves differently, the other partial cross sections scale essentially as the nucleon number. Final-state interactions obviously will destroy this scaling.

We have compared our predictions with the available experimental data. Our ratio for the coherent pion production over the total neutrino cross section is just compatible with the experimental upper limit. Another test concerns the ratio for charged currents π^+ production to the quasielastic cross section. A delicate point in the experiments concerns the definition of a quasielastic process and its separation from np-nh that the experiment does not distinguish. In one set of data a correction is applied to obtain a genuine quasielastic cross section and it is corrected as well for final-state interaction. In another set of results a generalized quasielastic is introduced, defined as events with only one lepton. In this case our 2p-2h and 3p-3h should be added to the quasielastic component. Both lead to successful comparisons with the two sets of experimental data. Further data involve a ratio of neutral current π^0 production to the total neutrino cross section for charged currents. Here again our evaluation agrees with data. It is quite encouraging that the comparison with present experimental data is essentially successful.

A distinct feature of our approach, and one of our significant results, is the large 2p-2h component. It affects all the measured ratios discussed in this work. At the present level of accuracy we have not found in these ratios any contradiction to its presence. It is also supported by preliminary data on the absolute neutrino quasielastic cross section on carbon. We suggest that the proposed increase of the axial mass from the standard value to a larger one to account for the quasielastic data, reflects the presence of a polarization cloud, mostly due to tensor interaction, which surrounds a nucleon in the nuclear medium. It translates into a final state with ejection of two nucleons, which in the present stage of the experiments is indistinguishable from the quasielastic final state. Although the existence of such 2p-2h component is not in question, for a fully quantitative evaluation we plan to improve the description of the multinucleon final states by a microscopic treatment. Future precision experiments, such as T2K, will be able to identify final states, namely p-p pairs for charged current and n-p pairs for neutral current and bring an experimental elucidation of this intriguing effect.

ACKNOWLEDGMENTS

We thank Luis Alvarez-Ruso, Dany Davesne, Torleif Ericson, and Alfredo Molinari for stimulating discussions.

APPENDIX A: INCLUSIVE NEUTRINO-NUCLEUS CROSS-SECTION

The invariant amplitude for the lepton-nucleus cross section, Eq. (1), results from the contraction between the leptonic L and the hadronic H tensors

$$|T|^2 = L_{00}W^{00} + L_{33}W^{33} + (L_{03} + L_{30})W^{03} + (L_{11} + L_{22})W^{11} \pm (L_{12} - L_{21})W^{12} \begin{cases} + & (\nu) \\ - & (\bar{\nu}) \end{cases}. \quad \text{(A1)}$$

The various L are the component of the leptonic tensor

$$L_{\mu\nu} = 8(k_\mu k'_\nu + k_\nu k'_\mu - g_{\mu\nu} k.k' \mp i\varepsilon_{\mu\nu\alpha\beta} k^\alpha k'^\beta) \quad \text{(A2)}$$

while the W of the hadronic one

$$W^{\mu\nu} = \sum_{P,P'=N,\Delta} \sqrt{\frac{M_P}{E_P^q}}\sqrt{\frac{M_{P'}}{E_{P'}^q}} H^{\mu\nu}_{PP'} = \frac{M_N}{E_N^q} H^{\mu\nu}_{NN} + \sqrt{\frac{M_N}{E_N^q}}\sqrt{\frac{M_\Delta}{E_\Delta^q}} H^{\mu\nu}_{N\Delta} + \frac{M_\Delta}{E_\Delta^q} H^{\mu\nu}_{\Delta\Delta}, \quad \text{(A3)}$$

where $E_N^q = (q^2 + {M_N}^2)^{1/2}$ and $E_\Delta^q = (q^2 + {M_\Delta}^2)^{1/2}$. This decomposition takes into account the different channels of particle-hole excitations. The various leptonic tensor components are:

$$\begin{aligned} L_{00} &= 8(k_0 {k'}_0 + k k' \cos\theta), \\ L_{33} &= 8(2k_3 {k'}_3 + k_0 {k'}_0 - k k' \cos\theta), \\ L_{03} + L_{30} &= 16(k_0 {k'}_3 + k_3 {k'}_0), \\ L_{11} + L_{22} &= 16\left(2k_1^2 + k_0 {k'}_0 - k k' \cos\theta\right), \\ L_{12} - L_{21} &= -i8(k_0 {k'}_3 - k_3 {k'}_0), \\ \text{with} \quad k_3 &= \frac{k}{q}(k' \cos\theta - k), \\ {k'}_3 &= \frac{k'}{q}(k' - k\cos\theta), \\ \text{and} \quad k_1 = k_2 &= \frac{k k'}{q}\frac{\sin\theta}{\sqrt{2}}. \end{aligned} \quad \text{(A4)}$$

For the hadronic tensor components we keep only the leading terms in the development of the hadronic current in p/M, where p denotes the initial nucleon momentum. Marteau investigated the importance of the momentum terms and found them to be small. The components are related to the various nuclear responses R as follows

$$\begin{aligned} H^{00}_{PP'} &= \alpha^0_P \alpha^0_{P'} R_\tau + \beta^0_P \beta^0_{P'} R_l \\ H^{03}_{PP'} &= \alpha^0_P \alpha^3_{P'} R_\tau + \beta^0_P \beta^3_{P'} R_l \\ H^{33}_{PP'} &= \alpha^3_P \alpha^3_{P'} R_\tau + \beta^3_P \beta^3_{P'} R_l \\ H^{11}_{PP'} &= \gamma^0_P \gamma^0_{P'} R_t + \delta^0_P \delta^0_{P'} R_t \\ H^{22}_{PP'} &= H^{11}_{PP'}, \\ H^{12}_{PP'} &= -i\gamma^0_P \delta^0_{P'} R_t - i\delta^0_P \gamma^0_{P'} R_t. \end{aligned} \quad \text{(A5)}$$

For sake of illustration we give the explicit expression of H^{00}:

$$H^{00} = \sum_{P,P'=N,\Delta} H^{00}_{PP'} = \alpha^0_N \alpha^0_N R^{NN}_\tau + \beta^0_N \beta^0_N R^{NN}_l + 2\beta^0_N \beta^0_\Delta R^{N\Delta}_l + \beta^0_\Delta \beta^0_\Delta R^{\Delta\Delta}_l. \quad \text{(A6)}$$

The quantities α, β, γ, and δ are expressed in terms of the usual form factors, namely

$$\begin{aligned} \alpha^0_P &= N^q_P \left[F_1 - F_2 \frac{\boldsymbol{q}^2}{2M_P\left(E^q_P + M_P\right)}\right], \\ \alpha^3_P &= N^q_P \left[F_1 - F_2 \frac{\omega}{2M_N}\right] \frac{|\boldsymbol{q}|}{E^q_P + M_P}, \\ \beta^0_P &= N^q_P \left[G^*_A - G_P \frac{\omega}{2M_N}\right] \frac{|\boldsymbol{q}|}{E^q_P + M_P}, \\ \beta^3_P &= N^q_P \left[G_A - G_P \frac{\boldsymbol{q}^2}{2M_N\left(E^q_P + M_P\right)}\right], \\ \gamma^0_P &= N^q_P \left[F_1 - F_2 \frac{\omega}{2M_N} + F_2 \frac{E^q_P + M_P}{2M_P}\right] \frac{|\boldsymbol{q}|}{E^q_P + M_P}, \\ \delta^0_P &= -N^q_P G_A. \end{aligned} \quad \text{(A7)}$$

We have introduced in the time component of the axial current a renormalization factor $G^*_A = G_A(1+\delta)$ to account meson exchange effects that are known to be important in this channel [68]. Even with the large value $\delta = 0.5$ the effect of this renormalization is small. The most affected channel is the coherent, which is reduced by $\simeq$10%.

1. Spin longitudinal contribution to the quasielastic cross section

We consider the limit of vanishing lepton mass. In this case the relevant leptonic tensor components reduce to

$$L_{00} = 4[(k+k')^2 - q^2] = \frac{q^2}{\omega^2} L_{33} = -\frac{1}{2}\frac{q}{\omega}(L_{03} + L_{30}). \quad \text{(A8)}$$

The longitudinal contribution to the quantity $|T|^2$ involves

$$\begin{aligned} &{\beta^0_N}^2 L_{00} + {\beta^3_N}^2 L_{33} + \beta^0_N \beta^3_N (L_{00} + L_{33}) \\ &\quad = {N^q_N}^2 G_A^2 L_{00} \left[\frac{q^2}{\left(E^q_N + M_N\right)^2} + \frac{\omega^2}{q^2} - 2\frac{\omega}{q}\frac{|\boldsymbol{q}|}{E^q_N + M_N}\right]. \end{aligned} \quad \text{(A9)}$$

Neglecting the struck nucleon momentum, the transferred energy ω in a quasielastic process is $\omega = E^q_N - M_N$, which implies the bracket on the right-hand side of Eq. (A9) to vanish.

APPENDIX B: PARTICLE-HOLE POLARIZATION PROPAGATORS

1. Bare

In this Appendix we give the expressions of the bare particle-hole polarization propagators. The nucleon-hole polarization propagator is the standard Lindhard function [86]. For the Δ-hole polarization propagator we use the relativistic expression

$$\Pi_{\Delta-\mathrm{h}}(q) = \frac{32\tilde{M}_\Delta}{9} \int \frac{d^3k}{(2\pi)^3}\theta(k_F - k) \times \left[\frac{1}{s - \tilde{M}^2_\Delta + i\tilde{M}_\Delta \Gamma_\Delta} - \frac{1}{u - \tilde{M}^2_\Delta}\right], \quad \text{(B1)}$$

where s and u are the Mandelstam variables. $\tilde{M}_\Delta = M_\Delta + 40(MeV)\frac{\rho}{\rho_0}$ is the mass of the Δ in the nuclear medium and Γ_Δ is the in medium Δ width. The last two quantities are taken from Ref. [70].

For the 2p-2h polarization propagators we consider only the imaginary parts. Their expressions, which represent an extrapolation of threshold results of [72] are

$$\mathrm{Im}\left(\Pi^0_{NN}\right) = 4\pi\rho^2 \frac{(2M_N + m_\pi)^2}{(2M_N + \omega)^2} C_1 \Phi_1(\omega)\left[\frac{1}{\omega^2}\right]$$

$$\mathrm{Im}\left(\Pi^0_{N\Delta}\right) = -4\pi\rho^2 \frac{(2M_N + m_\pi)^2}{(2M_N + \omega)^2} C_2 \Phi_2(\omega)\mathrm{Re}$$

$$\times\left[\frac{1}{\omega\left(\omega-\tilde{M}_\Delta+M_N+i\frac{\Gamma_\Delta}{2}\right)}+\frac{1}{\omega(\omega+\tilde{M}_\Delta-M_N)}\right]$$

$$\mathrm{Im}\left(\Pi^0_{\Delta\Delta}\right)=-4\pi\rho^2\frac{(2M_N+m_\pi)^2}{(2M_N+\omega)^2}C_3\Phi_3(\omega)\times\left[\frac{1}{(\omega+\tilde{M}_\Delta-M_N)^2}\right]. \quad \text{(B2)}$$

The C_i constants are set to $C_1=0.045, C_2=0.08, C_3=0.06$, while the $\Phi_i(\omega)$ include phase space, pion, and ρ propagators.

2. RPA

Here we define the RPA expressions of the response functions for finite nuclei.

First we introduce the projection of the bare propagators on the Legendre's polynomials P_L through

$$\Pi^{0(L)}(\omega,q,q')=2\pi\int du\,P_L(u)\Pi^0(\omega,\boldsymbol{q},\boldsymbol{q}'),$$
$$\Pi^{0(L)}_{k_F(R)}(\omega,q,q')=2\pi\int du\,P_L(u)\Pi^0_{k_F(R)}\left(\omega,\frac{\boldsymbol{q}+\boldsymbol{q}'}{2}\right), \quad \text{(B3)}$$

where $q=|\boldsymbol{q}|, q'=|\boldsymbol{q}'|, u=\cos(\widehat{q},\widehat{q'})$. Starting from Eqs. (5) and (B3), after some algebraic manipulations, one obtains

$$\Pi^{0(L)}(\omega,q,q')=4\pi\sum_{l_1,l_2}(2l_1+1)(2l_2+1)\begin{pmatrix}l_1 & l_2 & L\\ 0 & 0 & 0\end{pmatrix}^2\times\int dR R^2 j_{l_1}(qR)j_{l_1}(q'R)\Pi^{0(l_2)}_{k_F(R)}(\omega,q,q') \quad \text{(B4)}$$

with the usual three-j symbol and l-order Bessel function $j_l(x)$. This is the starting point for the calculations of isovector and spin-isospin response functions.

The free isovector (or charge) response function can be expressed through

$$R^{0NN}_{cc}(\omega,q)=-\frac{\mathcal{V}}{\pi}\sum_J\frac{2J+1}{4\pi}\mathrm{Im}\left[\Pi^{0(J)}_{N\mathrm{h}}(\omega,q,q)\right]. \quad \text{(B5)}$$

The RPA isovector response function

$$R^{NN}_{cc}(\omega,q)=-\frac{\mathcal{V}}{\pi}\mathrm{Im}[\Pi_{cc_{NN}}(\omega,\boldsymbol{q},\boldsymbol{q}),]=-\frac{\mathcal{V}}{\pi}\sum_J\frac{2J+1}{4\pi}\mathrm{Im}\left[\Pi^{(J)}_{cc_{NN}}(\omega,q,q)\right], \quad \text{(B6)}$$

is obtained solving the following equation

$$\Pi^{(J)}_{cc_{NN}}(\omega,q,q')=\Pi^{0(J)}_{N\mathrm{h}}(\omega,q,q')+\int\frac{dkk^2}{(2\pi)^3}\Pi^{0(J)}_{N\mathrm{h}}(\omega,q,k)\times V^{NN}_c(k)\Pi^{(J)}_{cc_{NN}}(\omega,k,q'). \quad \text{(B7)}$$

For the spin-isospin longitudinal and transverse responses we introduce the following quantities

$$\Pi^{0(J)}_{ll_{PP'}}(\omega,q,q')=\sum_{L=J\pm1}a^2_{JL}\Pi^{0(L)}_{PP'}(\omega,q,q'),$$
$$\Pi^{0(J)}_{lt_{PP'}}(\omega,q,q')=\sum_{L=J\pm1}a_{JL}b_{JL}\Pi^{0(L)}_{PP'}(\omega,q,q'), \quad \text{(B8)}$$
$$\Pi^{0(J)}_{tt_{PP'}}(\omega,q,q')=\sum_{L=J\pm1}b^2_{JL}\Pi^{0(L)}_{PP'}(\omega,q,q').$$

where

$$a_{JL}=\begin{cases}-\sqrt{\frac{J}{2J+1}} & \text{for } L=J-1,\\ \sqrt{\frac{J+1}{2J+1}} & \text{for } L=J+1.\end{cases}$$
$$b_{JL}=\begin{cases}\sqrt{\frac{J+1}{2J+1}} & \text{for } L=J-1,\\ \sqrt{\frac{J}{2J+1}} & \text{for } L=J+1,\\ 1 & \text{for } L=J.\end{cases} \quad \text{(B9)}$$

Note that, in general, for finite systems $\Pi^{0(J)}_{lt}\neq0$. The bare responses in a particular channel k ($k=QE$, 2p-2h,...) are given by

$$R^{0PP'}_{(k)xy}(\omega,q)=-\frac{\mathcal{V}}{\pi}\sum_J\frac{2J+1}{4\pi}\mathrm{Im}\left[\Pi^{0(J)}_{(k)xy_{PP'}}(\omega,q,q)\right], \quad \text{(B10)}$$

with $x,y=l,t$, referred to the longitudinal or transverse channel, and $PP'=N,\Delta$.

The second term of Eq. (10) in the channel k, namely

$$\mathrm{Im}\Pi_{(k)}=|1+\Pi V|^2\,\mathrm{Im}\Pi^0_{(k)}, \quad \text{(B11)}$$

with Π the full polarization propagator, explicitly writes

$$\Pi^{(J)}_{(k)xy_{PP'}}(\omega,q,q')=\Pi^{0(J)}_{(k)xy_{PP'}}(\omega,q,q')+\int\frac{dpp^2}{(2\pi)^3}\sum_{\substack{QR\\ ww'}}\Pi^{0(J)}_{(k)xw_{PQ}}(\omega,q,p)\times V^{QR}_{ww'}(p)\Pi^{(J)}_{w'y_{QP'}}(\omega,p,q')+\int\frac{dpp^2}{(2\pi)^3}\sum_{\substack{QR\\ ww'}}\left[\Pi^{(J)}_{xw_{PQ}}(\omega,q,p)\times V^{QR}_{ww'}(p)\right]^*\Pi^{0(J)}_{(k)w'y_{QP'}}(\omega,p,q')+\int\int\frac{dpp^2}{(2\pi)^3}\frac{dp'p'^2}{(2\pi)^3}\sum_{\substack{QQ'RR'\\ ww'zz'}}\left[\Pi^{(J)}_{xw_{PR}}\times(\omega,q,p)V^{RQ}_{wz}(p)\right]^*\Pi^{0(J)}_{(k)zz'_{QQ'}}(\omega,p,p')\times V^{Q'R'}_{z'w'}(p')\Pi_{w'y_{R'P'}}(\omega,p',q'), \quad \text{(B12)}$$

where $x,y,w,w',z,z'=l$ or t and $P,P',Q,Q',R,R'=N,\Delta$. The solution of this equation leads to the corresponding response functions

$$R^{PP'}_{(k)xy}(\omega,q)=-\frac{\mathcal{V}}{\pi}\sum_J\frac{2J+1}{4\pi}\mathrm{Im}\left[\Pi^{(J)}_{(k)xy_{PP'}}(\omega,q,q)\right]. \quad \text{(B13)}$$

In our calculations the maximum multipole number is set to $J = 25$, which turns out to be sufficient to reach the convergence.

The first term of Eq. (10), which represents coherent processes, explicitly writes

$$\begin{aligned}\Pi^{(J)}_{(co.)_{xyP'P'}}(\omega, q, q') &= \int \frac{dpp^2}{(2\pi)^3}\left[\Pi^{(J)}_{xlPQ}(\omega, q, p)\right]^* \\ &\quad \times \mathrm{Im}\left[V_\pi^{QQ'}(p)\right]\Pi^{(J)0}_{lyQ'P'}(\omega, p, q') \\ &= -i\frac{q_\pi^2}{16\pi^2}\left\{\frac{f^2}{m_\pi^2}\left[\Pi^{(J)}_{xlPN}(\omega, q, q_\pi)\right]^*\right. \\ &\quad \times \Pi^{(J)}_{lyNP'}(\omega, q_\pi, q')\frac{ff^*}{m_\pi^2} \\ &\quad \times \left[\Pi^{(J)}_{xlPN}(\omega, q, q_\pi)\right]^*\Pi^{(J)}_{ly\Delta P'}(\omega, q_\pi, q') \\ &\quad + \frac{f^*f}{m_\pi^2}\left[\Pi^{(J)}_{xlP\Delta}(\omega, q, q_\pi)\right]^*\Pi^{(J)}_{lyNP'} \\ &\quad \times (\omega, q_\pi, q') + \frac{f^{*2}}{m_\pi^2}\left[\Pi^{(J)}_{xlP\Delta}(\omega, q, q_\pi)\right]^* \\ &\quad \left.\times\ \Pi^{(J)}_{ly\Delta P'}(\omega, q_\pi, q')\right\}, \end{aligned} \tag{B14}$$

where

$$\begin{aligned}\mathrm{Im}(V_\pi) &= \mathrm{Im}\left(C_\pi\frac{\boldsymbol{q}^2}{\omega^2 - \boldsymbol{q}^2 - m_\pi^2 + i\eta}\right) \\ &= -iC_\pi\pi\boldsymbol{q}^2\delta(\boldsymbol{q}^2 - q_\pi^2) = -iC_\pi\pi\frac{q_\pi}{2}\delta(|\boldsymbol{q}| - q_\pi), \end{aligned} \tag{B15}$$

with C_π the generic nucleon- or Δ-pion coupling constant and $q_\pi = \sqrt{\omega^2 - m_\pi^2}$.

[1] Y. Fukuda *et al.* (Super-Kamiokande Collaboration), Phys. Rev. Lett. **81**, 1562 (1998).
[2] A. A. Aguilar-Arevalo *et al.* (SciBooNE Collaboration), arXiv:hep-ex/0601022.
[3] A. A. Aguilar-Arevalo *et al.* (MiniBooNE Collaboration), Nucl. Instrum. Methods A **599**, 28 (2009).
[4] Y. Itow *et al.* (T2K Collaboration), arXiv:hep-ex/0106019.
[5] R. Terri (T2K Collaboration), Nucl. Phys. Proc. Suppl. **189**, 277 (2009).
[6] S. Nakayama *et al.* (K2K Collaboration), Phys. Lett. **B619**, 255 (2005).
[7] M. Hasegawa *et al.* (K2K Collaboration), Phys. Rev. Lett. **95**, 252301 (2005).
[8] R. Gran *et al.* (K2K Collaboration), Phys. Rev. D **74**, 052002 (2006).
[9] A. A. Aguilar-Arevalo *et al.* (MiniBooNE Collaboration), Phys. Rev. Lett. **100**, 032301 (2008).
[10] A. A. Aguilar-Arevalo *et al.* (MiniBooNE Collaboration), Phys. Lett. **B664**, 41 (2008).
[11] A. Rodriguez *et al.* (K2K Collaboration), Phys. Rev. D **78**, 032003 (2008).
[12] K. Hiraide *et al.* (SciBooNE Collaboration), Phys. Rev. D **78**, 112004 (2008).
[13] A. A. Aguilar-Arevalo *et al.* (MiniBooNE Collaboration), Phys. Rev. D **79**, 072002 (2009).
[14] A. A. Aguilar-Arevalo *et al.*, Phys. Rev. Lett. **103**, 081801 (2009).
[15] T. Katori (MiniBooNE Collaboration), AIP Conf. Proc. **1189**, 139 (2009).
[16] Y. Kurimoto (SciBooNE Collaboration), AIP Conf. Proc. **1189**, 189 (2009).
[17] J. L. Alcaraz-Aunion and J. Walding (SciBooNE Collaboration), AIP Conf. Proc. **1189**, 145 (2009).
[18] A. Kartavtsev, E. A. Paschos, and G. J. Gounaris, Phys. Rev. D **74**, 054007 (2006).
[19] S. K. Singh, M. S. Athar, and S. Ahmad, Phys. Rev. Lett. **96**, 241801 (2006).
[20] S. Ahmad, M. S. Athar, and S. K. Singh, Phys. Rev. D **74**, 073008 (2006).
[21] D. Rein and L. M. Sehgal, Phys. Lett. **B657**, 207 (2007).
[22] L. Alvarez-Ruso, L. S. Geng, S. Hirenzaki, and M. J. Vicente Vacas, Phys. Rev. C **75**, 055501 (2007); [Erratum-*ibid.* **80**, 019906 (2009)].
[23] L. Alvarez-Ruso, L. S. Geng, and M. J. Vicente Vacas, Phys. Rev. C **76**, 068501 (2007); [Erratum-*ibid.* **80**, 029904 (2009)].
[24] A. V. Butkevich, Phys. Rev. C **78**, 015501 (2008).
[25] C. Praet, O. Lalakulich, N. Jachowicz, and J. Ryckebusch, arXiv:0804.2750 [nucl-th].
[26] M. Sajjad Athar, S. Chauhan, and S. K. Singh, arXiv:0808.2103 [nucl-th].
[27] J. E. Amaro, E. Hernandez, J. Nieves, and M. Valverde, Phys. Rev. D **79**, 013002 (2009).
[28] T. Leitner, O. Buss, U. Mosel, and L. Alvarez-Ruso, Phys. Rev. C **79**, 038501 (2009).
[29] C. Berger and L. M. Sehgal, Phys. Rev. D **79**, 053003 (2009).
[30] T. Leitner, U. Mosel, and S. Winkelmann, Phys. Rev. C **79**, 057601 (2009).
[31] E. A. Paschos and D. Schalla, Phys. Rev. D **80**, 033005 (2009).
[32] O. Benhar and D. Meloni, Phys. Rev. D **80**, 073003 (2009).
[33] E. Hernandez, J. Nieves, and M. J. Vicente Vacas, Phys. Rev. D **80**, 013003 (2009).
[34] A. V. Butkevich, Phys. Rev. C **80**, 014610 (2009).
[35] M. S. Athar, S. Chauhan, and S. K. Singh, arXiv:0908.1442 [nucl-th].
[36] S. X. Nakamura, T. Sato, T. S. Lee, B. Szczerbinska, and K. Kubodera, arXiv:0910.1057 [nucl-th].
[37] J. Delorme and M. Ericson, Phys. Lett. **B156**, 263 (1985).
[38] J. Marteau, Eur. Phys. J. A **5**, 183 (1999).
[39] J. Marteau, J. Delorme, and M. Ericson, Nucl. Instrum. Methods A **451**, 76 (2000).
[40] S. K. Singh and E. Oset, Nucl. Phys. **A542**, 587 (1992).
[41] S. K. Singh and E. Oset, Phys. Rev. C **48**, 1246 (1993).
[42] L. Alvarez-Ruso, S. K. Singh, and M. J. Vicente Vacas, Phys. Rev. C **57**, 2693 (1998).
[43] S. K. Singh, M. J. Vicente-Vacas, and E. Oset, Phys. Lett. **B416**, 23 (1998); [Erratum-*ibid.* **B423**, 428 (1998)].
[44] T. Sato, D. Uno, and T. S. H. Lee, Phys. Rev. C **67**, 065201 (2003).
[45] B. Szczerbinska, T. Sato, K. Kubodera, and T. S. Lee, Phys. Lett. **B649**, 132 (2007).

[46] E. A. Paschos, J. Y. Yu, and M. Sakuda, Phys. Rev. D **69**, 014013 (2004).
[47] A. Meucci, C. Giusti, and F. D. Pacati, Nucl. Phys. **A739**, 277 (2004).
[48] A. Meucci, C. Giusti, and F. D. Pacati, Nucl. Phys. **A744**, 307 (2004).
[49] J. Nieves, J. E. Amaro, and M. Valverde, Phys. Rev. C **70**, 055503 (2004); [Erratum-*ibid.* **72**, 019902 (2005)].
[50] J. E. Amaro, M. B. Barbaro, J. A. Caballero, T. W. Donnelly, A. Molinari, and I. Sick, Phys. Rev. C **71**, 015501 (2005).
[51] J. A. Caballero, J. E. Amaro, M. B. Barbaro, T. W. Donnelly, C. Maieron, and J. M. Udias, Phys. Rev. Lett. **95**, 252502 (2005).
[52] J. E. Amaro, M. B. Barbaro, J. A. Caballero, and T. W. Donnelly, Phys. Rev. Lett. **98**, 242501 (2007).
[53] M. Martini, G. Co', M. Anguiano, and A. M. Lallena, Phys. Rev. C **75**, 034604 (2007).
[54] J. E. Amaro, M. B. Barbaro, J. A. Caballero, T. W. Donnelly, and J. M. Udias, Phys. Rev. C **75**, 034613 (2007).
[55] M. V. Ivanov, M. B. Barbaro, J. A. Caballero, A. N. Antonov, E. Moya de Guerra, and M. K. Gaidarov, Phys. Rev. C **77**, 034612 (2008).
[56] M. C. Martinez, P. Lava, N. Jachowicz, J. Ryckebusch, K. Vantournhout, and J. M. Udias, Phys. Rev. C **73**, 024607 (2006).
[57] O. Benhar, N. Farina, H. Nakamura, M. Sakuda, and R. Seki, Phys. Rev. D **72**, 053005 (2005).
[58] O. Benhar and D. Meloni, Phys. Rev. Lett. **97**, 192301 (2006).
[59] O. Benhar and D. Meloni, Nucl. Phys. **A789**, 379 (2007) .
[60] A. M. Ankowski and J. T. Sobczyk, Phys. Rev. C **74**, 054316 (2006).
[61] T. Leitner, L. Alvarez-Ruso, and U. Mosel, Phys. Rev. C **73**, 065502 (2006).
[62] T. Leitner, L. Alvarez-Ruso, and U. Mosel, Phys. Rev. C **74**, 065502 (2006).
[63] E. Hernandez, J. Nieves, and M. Valverde, Phys. Rev. D **76**, 033005 (2007).
[64] T. Leitner, O. Buss, L. Alvarez-Ruso, and U. Mosel, Phys. Rev. C **79**, 034601 (2009).
[65] J. Delorme and P. A. M. Guichon, Phys. Lett. **B263**, 157 (1991).
[66] W. M. Alberico, M. Ericson, and A. Molinari, Annals Phys. **154**, 356 (1984).
[67] A. De Pace, M. Nardi, W. M. Alberico, T. W. Donnelly, and A. Molinari, Nucl. Phys. **A726**, 303 (2003).
[68] K. Kubodera, J. Delorme, and M. Rho, Phys. Rev. Lett. **40**, 755 (1978).
[69] G. F. Low *et al.*, Phys. Rev. **106**, 1345 (1957).
[70] E. Oset and L. L. Salcedo, Nucl. Phys. **A468**, 631 (1987).
[71] J. Delorme and P. A. M. Guichon, in *Proceedings of* 10^{e} *Biennale de Physique Nucléaire, Aussois, France, 6–10 March 1989*, LYCEN report 8906, p. C.4.1, also in the *Proceedings of the 5th French-Japanese Symposium on Nuclear Physics, Dogashima, Izu, 26–30 September 1989*, edited by K. Shimizu and O. Hashimoto (University of Tokio Press, Tokio, 1990), p. 66.
[72] K. Shimizu and A. Faessler, Nucl. Phys. **A333**, 495 (1980).
[73] H. De Vries, C. W. De Jager, and C. De Vries, At. Data Nucl. Data Tables **36**, 495 (1987).
[74] M. Ichimura, H. Sakai, and T. Wakasa, Progr. Part. Nucl. Phys. **56**, 446 (2006).
[75] T. E. O. Ericson and W. Weise, *Pions and Nuclei, The International Series of Monographs on Physics* (Clarendon, Oxford, UK, 1988), Vol. 74, p. 479.
[76] D. Ashery, I. Navon, G. Azuelos, H. K. Walter, H. J. Pfeiffer, and F. W. Schleputz, Phys. Rev. C **23**, 2173 (1981).
[77] S. L. Adler, Phys. Rev. **135**, B963 (1964).
[78] S. Boyd, S. Dytman, E. Hernández, J. Sobczyk, and R. Tacik, AIP Conf. Proc. **1189**, 60 (2009).
[79] M. Ericson and T. E. O. Ericson, Annals Phys. **36**, 323 (1966).
[80] D. Rein and L. M. Sehgal, Nucl. Phys. **B223**, 29 (1983).
[81] J. L. Raaf, Ph.D. thesis, University of Cincinnati, 2005.
[82] G. M. Radecky *et al.*, Phys. Rev. D **25**, 1161 (1982); [Erratum-*ibid.* **26**, 3297 (1982)].
[83] J. M. Laget, Nucl. Phys. **A358**, 275C (1981).
[84] O. Benhar, A. Fabrocini, S. Fantoni, A. Y. Illarionov, and G. I. Lykasov, Phys. Rev. C **67**, 014326 (2003).
[85] M. J. Vicente Vacas, M. K. Khankhasaev, and S. G. Mashnik, arXiv:nucl-th/9412023.
[86] A. L. Fetter and J. D. Walecka, *Quantum Theory of Many-Particle Systems* (McGraw-Hill, New York, 1971).